



## **Design of permanent-magnet solenoids with finite-element methods**

Stanley Humphries, Ph.D.

**Field Precision LLC**

E mail: [techinfo@fieldp.com](mailto:techinfo@fieldp.com)

Internet: <https://www.fieldp.com>

# 1 Introduction

A *solenoid* is a cylindrical region of approximately uniform axial magnetic flux density ( $B_z$ ). In accelerator applications, solenoids are employed to confine or to focus high-current electron beams. They are also used in plasma ion sources. Large-volume solenoid fields are generated with current-carrying coils (normal or superconducting). Permanent magnets have the advantages that do not require a current supply and cooling. On the other hand, the atomic current distributions of permanent magnets are not ideal for solenoid-type fields and present definite limitations. In this tutorial, I will review some features of solenoids using modern permanent-magnet materials (such as neodymium iron and samarium cobalt). I will also discuss several field solutions with **PerMag** that illustrate the range of field magnitude and uniformity in practical solenoids. The final section describes a method for designing permanent-magnet magnetic mirror fields with a specified mirror ratio.

A conventional solenoid consists of an azimuthal winding of current-carrying wires on a cylindrical mandrel, as shown in Fig. 1a<sup>1</sup>. Current in the shaded coil region flows out of the page. The term *solenoid* comes from the Greek word for pipe because the coil acts as a conduit for magnetic flux. The magnitude of the flux density is approximately uniform inside the coil. The flux returns through the surrounding air volume. The addition of an iron flux-return structure (Fig. 1b) improves the performance of a conventional solenoid. The iron localizes the field and reduces reluctance of the magnetic circuit. As a result, the internal flux is more uniform and the magnitude  $B_z(0,0)$  is close to the value for an infinite-length solenoid. For a given field magnitude, the solenoid of Fig. 1b requires only 80% of the power for a bare coil.

The basic physical properties of ferromagnetic materials are described in Chap. 5 of the text S. Humphries, **Principles of Charged Particle Acceleration** (Wiley-Interscience, New York, 1986). The book is freely available for download at:

<http://www.fieldp.com/cpa.html>

The magnetic domains in modern permanent-magnet materials are aligned and rigidly locked. Atomic currents flow in a direction normal to the axis of magnetization. The summation of atomic currents gives zero current inside the material and a current layer on the material surface. An infinite-length bar of permanent-magnet material has a line current density  $J_s$  A/m. The flux density outside the bar approaches zero, and the internal value is

---

<sup>1</sup>All illustrations in this report are  $z$ - $r$  plots, not sections in the  $x$  or  $y$  planes. Only positive values of  $r$  are defined

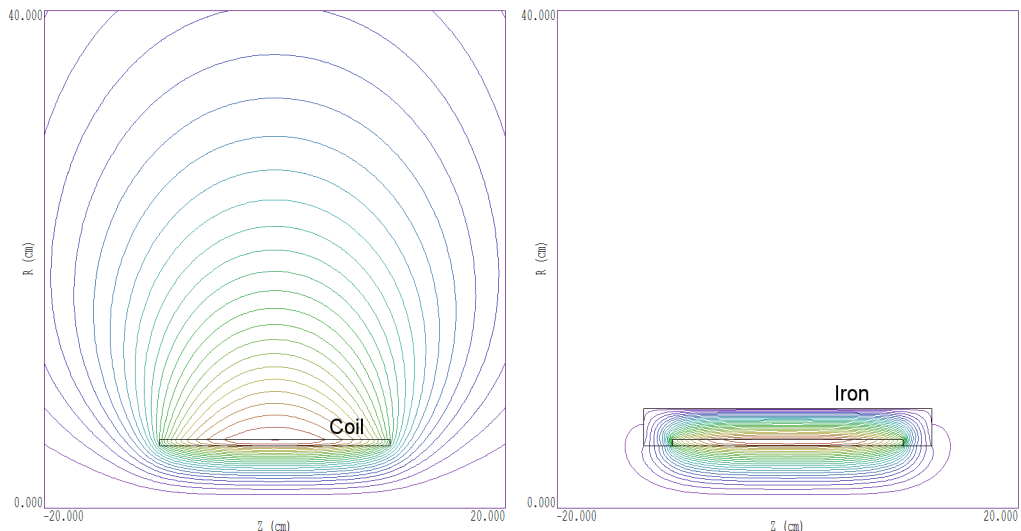


Figure 1: Calculated lines of magnetic flux density  $\mathbf{B}$  produced by a solenoid coil with radius  $R = 5.25$  cm, length  $L = 20.0$  cm and line current  $J_s = 9.018 \times 10^4$  A/m. *a)* Bare coil,  $B_z(0,0) = 0.1000$  tesla. *b)* iron shield,  $B_z(0,0) = 0.1112$  tesla.

$$B_r = \mu_0 J_s. \quad (1)$$

The quantity  $B_r$  is called the *remanence* flux density. The values of  $B_r$  for neodymium-iron magnets are in the range  $1.0 \rightarrow 1.4$  tesla.

If we limit attention to cylindrically-symmetric systems, permanent magnets for solenoid fields must be magnetized in either the axial ( $z$ ) or radial ( $r$ ) direction. In charged-particle applications, the region near the axis must be free of materials. Therefore, the permanent magnet must have the shape of an annulus. Figure 2 shows lines of  $\mathbf{B}$  for an annular magnet with axial magnetization. The summation of atomic currents gives uniform line current densities pointing in the  $+\theta$  direction on the inside and  $-\theta$  direction on the outside, with magnitude given by Eq. 1. In contrast to the solenoid coil of Fig. 1*a*, the dual current layers work against each other. There are two implications:

- The internal flux approaches zero as the axial length of the magnet increases.
- Flux utilization from a finite-length magnet is relatively inefficient.

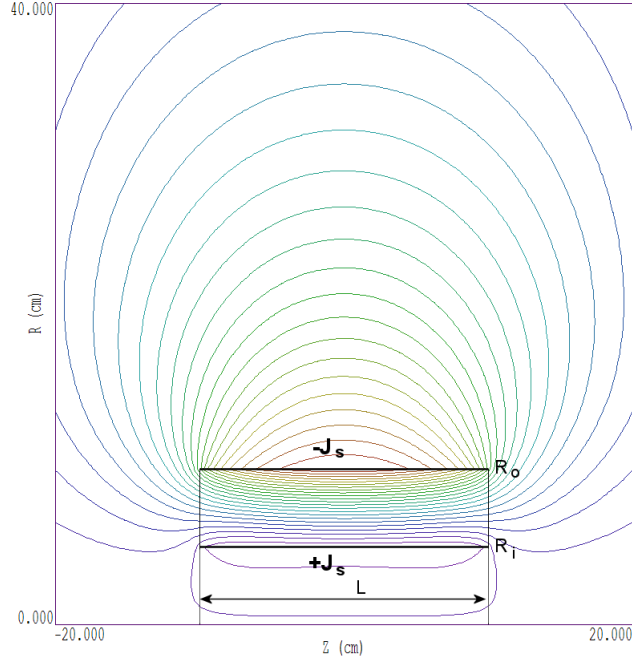


Figure 2: Lines of  $\mathbf{B}$  generated by a finite-length, annular permanent magnet with axial magnetization.

## 2 Solenoid field – axial magnetization

We shall start by investigating the type of solenoid field generated by annular permanent magnets with axial magnetization of the type shown in Fig. 2. In the demonstration calculations, we shall take  $B_r = 1.0$  tesla. A significant theoretical advantage of a modern permanent magnet is that its state is almost unaffected by other magnets and applied fields. There are two implications:

- The total flux density of an array of magnets is the linear superposition of individual values of  $\mathbf{B}$ .
- The total external magnetic flux density is linearly proportional to  $B_r$ .

To simplify the calculations, the cross-sections of magnets are rectangular. Chamfers and fillets introduce only small relative differences.

The geometry of Fig. 2 has two independent parameters:  $R_o/R_i$  and  $L/R_i$ , where  $R_i$  is the inner radius of the annulus,  $R_o$  is the outer radius and  $L$  is the axial length. The choice  $R_i = 5.0$  cm was used in all calculations. Field values apply to other systems if all dimensions are scaled by the same factor.

Table 1: Annular magnet with axial magnetization – variation with length ( $B_r = 1.0$  tesla,  $R_i = 5.0$  cm,  $R_o = 10.0$  cm).

$L$ (cm)	$B_z(0, 0)$ (tesla)	$U_{in}/U_{tot}$	$V$ (cm <sup>3</sup> )
10.0	-0.260	12.1%	2356
15.0	-0.234	10.0%	3534
20.0	-0.191	8.4%	4712
30.0	-0.122	6.5%	7068

The calculation of Fig. 2 was performed with  $R_o = 2R_i = 10.0$  cm and  $L = 4R_i = 20.0$  cm. To simulate a free space boundary, a large solution volume was used for the **PerMag** calculation with coarse element resolution outside the magnet region. The internal field was  $B_z(0, 0) = -0.1942$  tesla. We can arrive at the same field values by replacing the permanent magnet with uniform current layers. A confirming calculation has a positive current layer of length 20 cm between  $r = 4.75$  and 5.25 cm and a negative layer between 9.75 cm and 10.25 cm. The drive currents are

$$I = \pm \frac{B_r L}{\mu_0} = \pm 1.5916 \times 10^5 \text{ A.} \quad (2)$$

The implication for theoretical work is that a modern permanent magnets can be replaced by thin layers where the direction of the current is normal to the magnetization axis, The linear current density is given by Eq. 1. Another important point is that an iron shield cannot be used to carry external return 1b. We can shown with **PerMag** that an iron shell around the outer radius provides a low reluctance path that carries almost all the flux produced by the magnet, reducing the internal field close to zero.

In the first production run, the length  $L$  was varied with fixed  $R_o/R_i = 2.0$ . To compare field energy utilization, the air volume was divided into two regions: the interior of the solenoid and the remaining volume. Table 1 summarizes the results. Field cancellation between the inner and outer current layers increases with the magnet length. In consequence, the midplane field  $B_z(0, 0)$  as well as the energy utilization ratio decreases with higher  $L$ . In the table, the quantity  $U_{in}$  is the electrostatic field energy in the cylindrical bore of the magnet and  $U_{tot}$  is the total field energy in air. Figure 3 shows plots of  $B_z(z, 0)$ . For the axially-uniform magnet with  $R_o/R_i = 2.0$ , the best length for field uniformity is  $L/R_i \cong 4.0$ . For this choice, the length of the uniform field region is about  $2.0R_i$  (or  $L/2.0$ ) with field magnitude  $|B_z(0, 0)|/B_r = 0.191$ .

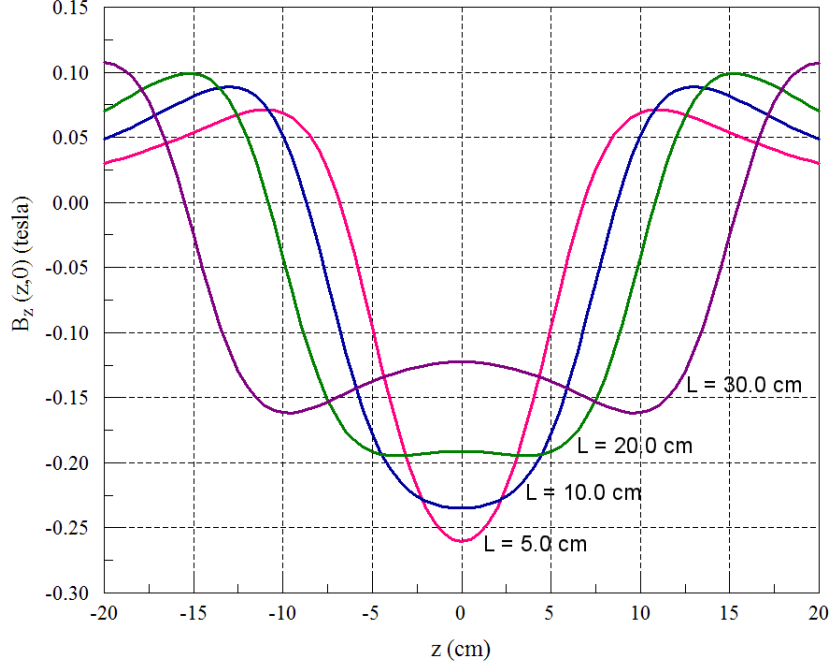


Figure 3: Variation of  $B_z(z, 0)$  with magnet length  $L$  ( $B_r = 1.0$  tesla,  $R_i = 5.0$  cm,  $R_o = 10.0$  cm).

In the second run (PMSOLE06), the outer radius  $R_o$  was varied with fixed length  $L = 4.0R_i$ . The results are listed in Table 2. Higher fields can be achieved at the expense of a larger magnet volume and reduced energy utilization. In the limit  $R_o \rightarrow \infty$ , the outer current layer is removed to infinity and the calculation becomes identical to that of Fig. 1a. From the result we can conclude that the limiting value of  $B_z(0, 0)$  for an infinite radius magnet with  $L/R_i = 4.0$  is  $0.885B_r$ .

Table 2: Annular magnet with axial magnetization – variation with outer radius ( $B_r = 1.0$  tesla,  $R_i = 5.0$  cm,  $L = 20.0$  cm).

$R_o$ (cm)	$B_z(0, 0)$ (tesla)	$U_{in}/U_{tot}$	$V$ (cm <sup>3</sup> )
10.0	-0.190	8.5%	4712
15.0	-0.347	6.6%	12566
20.0	-0.461	5.5%	23561
25.0	-0.545	4.7%	37699

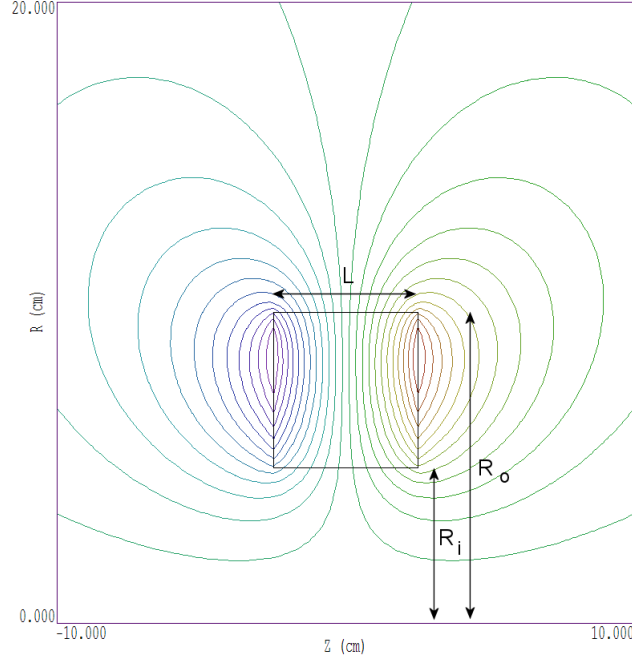


Figure 4: Lines of  $\mathbf{B}$  for an annular permanent magnet with radial magnetization ( $R_i = 5.0$  cm,  $R_o = 10.0$  cm,  $L = 5.0$  cm).

### 3 Magnetic mirror – radial magnetization

A magnetic mirror is a solenoid field that increases axially away from a mid-plane before dropping off at large distance. The field variation for  $L = 30.0$  cm in Fig. 3 is an example of a mirror-type field. An important parameter for plasma confinement is the mirror ratio,

$$M = \frac{B_{max}}{B_{min}}, \quad (3)$$

where  $B_{min} = B_z(0, 0)$  and  $B_{max}$  is highest field value. The calculations of the previous section demonstrate that large values of  $M$  cannot be achieved with axial magnetization. As an alternative, we shall consider assemblies of annular magnets with radial magnetization. To begin, it is useful to understand the fields from a single magnet – Fig. 4 shows the geometry and definitions of quantities.

Figure 5 shows the field variation  $B_z(z, 0)$  for a single radial magnet, with the origin of the  $z$  axis at the magnet center. A magnetic mirror field can be created with two magnets with inward and outward radial magnetization separated by an axial distance. The mirror ratio depends on the choice of separation distance. For guidance in the choice, we shall characterize the field variations of a single radial magnet with different choices of  $R_o/R_i$  and

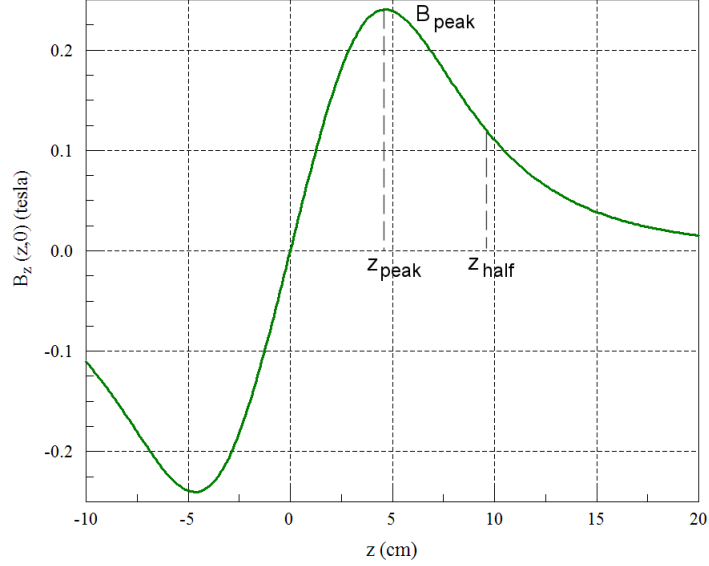


Figure 5: Variation  $B_z(z, 0)$  for an annular permanent magnet with radial magnetization ( $R_i = 5.0$  cm,  $R_o = 10.0$  cm,  $L = 7.5$  cm).

Table 3: Annular magnet with radial magnetization – variation with length ( $B_r = 1.0$  tesla,  $R_i = 5.0$  cm,  $R_o = 10.0$  cm).

$L$ (cm)	$B_{peak}$ (tesla)	$z_{peak}$	$z_{half} - z_{peak}$
2.5	0.0996	3.50	4.70
5.0	0.1820	3.90	4.85
7.5	0.2403	4.70	4.90
10.0	0.2779	5.60	5.00

$L/R_i$ . Table 3 shows results where  $L/R_i$  varies and  $R_o/R_i$  has the fixed value 2.0. The value of  $B_{peak}$  rises simply because there is more available flux with a larger magnet cross-section. With the given aspect ratio, the peak flux density is about one-third  $B_r$ . The axial extent of the field region has little dependence on  $L$ . Table 4 shows results with a variation of  $R_o/R_i$  at fixed  $L/R_i$ . There is a modest increase of peak field at the expense of a much larger magnet volume. As expected, the axial extent of the field increases with the average magnet radius.

Two separated magnets with oppositely-directed radial magnetization create a region of axial flux density (Fig. 6). With modern magnetic materials, the total field in the absence of iron is the superposition of fields from the individual magnets. The calculations listed in Tables 3 and 4 give the



Table 4: Annular magnet with radial magnetization – variation with outer radius ( $B_r = 1.0$  tesla,  $R_i = 5.0$  cm,  $L = 5.0$  cm).

$R_o$ (cm)	$B_{peak}$ (tesla)	$z_{peak}$	$z_{half} - z_{peak}$
10.0	0.1820	3.90	4.85
12.5	0.2186	4.20	5.30
15.0	0.2416	4.38	6.30
17.5	0.2570	4.50	6.30
20.0	0.2676	5.00	6.30

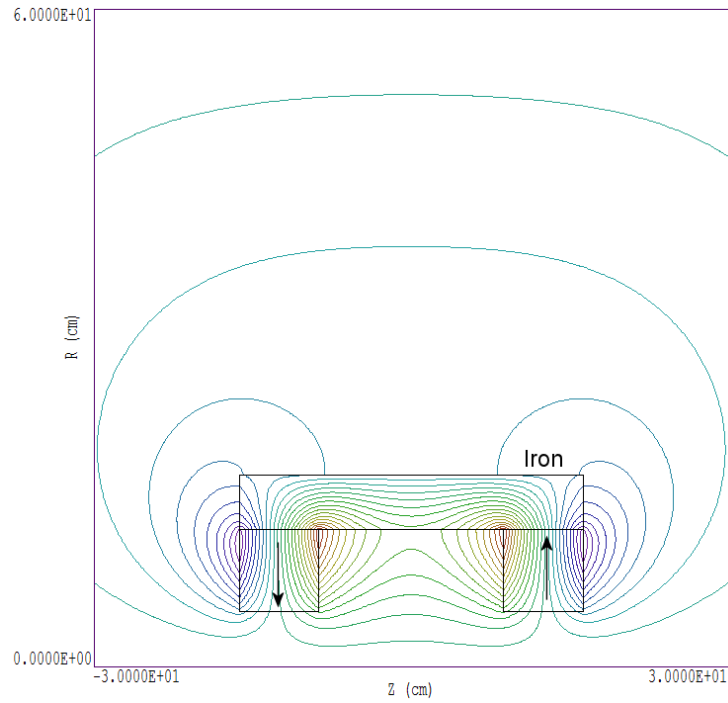


Figure 6: Magnetic mirror created with two axially-separated annular magnets with oppositely-directed radial magnetization. The iron pipe reduces the circuit reluctance.

Table 5: Annular magnet with radial magnetization – variation with outer radius ( $B_r = 1.0$  tesla,  $R_i = 5.0$  cm,  $L = 5.0$  cm).

$z$ (cm)	$\zeta$ (cm)	$B_z$ (tesla)	$f(\zeta)$
4.80	0.0	0.2942	1.000
12.50	$D/2.0$	0.09897	0.336
20.20	$D$	0.0260	0.088

variation of magnetic field as a function of distance from the peak field point,

$$B_z(\zeta, 0) = B_{peak}f(\zeta). \quad (4)$$

Let  $D$  be the distance between the two positions of maximum flux density. Combining two magnets, the maximum flux density is  $B_{max} = B_{peak}f(1 + D)$  and the minimum is  $B_{min} = 2B_{peak}f(D/2)$ . The mirror ratio is

$$M = \frac{1 + f(D)}{2 f(D/2)}. \quad (5)$$

An inspection of the results of Table 3 show that  $M > 1$  when  $D$  exceeds about 10 cm.

A test calculation employed magnets with dimensions  $R_i = 5.0$  cm,  $R_o = 10.0$  cm and  $L = 7.50$  cm. A scan of  $B_z(z, 0)$  shows that  $B_z = 0.2942$  tesla at  $z = 4.80$  cm. An assembly with two magnets with an axial separation of 25.0 cm corresponds to  $D = 25.0 - 2.0 \times 4.8 = 15.40$  cm. The field scan gives the values listed in Table 5. Substitution in Eq. 5 gives  $M = 1.62$ . A field calculation with the region outside the magnets in Fig. 6 set to  $\mu_r = 1.0$  gives the variation  $B_z(z, 0)$  shown as a black line in Fig. 7. In general, the peak  $|\mathbf{B}|$  in a practical assembly will be in the range  $\leq B_r/2$ . To achieve higher fields than those in Fig. 7, we could use a material with larger  $B_r$  or increase  $R_o/R_i$  or  $L/R_i$ . In either case, there will be a penalty in terms of the cost and difficulty of handling the magnets. Finally, some applications require an asymmetric magnetic mirror. In this case we could use magnets with different values for  $R_o/R_i$  and/or  $L/R_i$ .

An iron shield is beneficial in the radial magnet configuration. Iron can carry some of the external flux between magnets, reducing the reluctance of the circuit. For the field configuration in Fig. 6, the outer shield had the property  $\mu_r = 1000.0$ . The resulting variation  $B_z(z, 0)$  is plotted as the blue trace in Fig. 7. The effect of iron is to increase the on-axis field by about 13%. A final issue is how to choose the thickness of the iron shield. The material should not be saturated – the solution almost independent of detailed material properties as long as  $\mu_r \gg 1.0$  throughout. In the

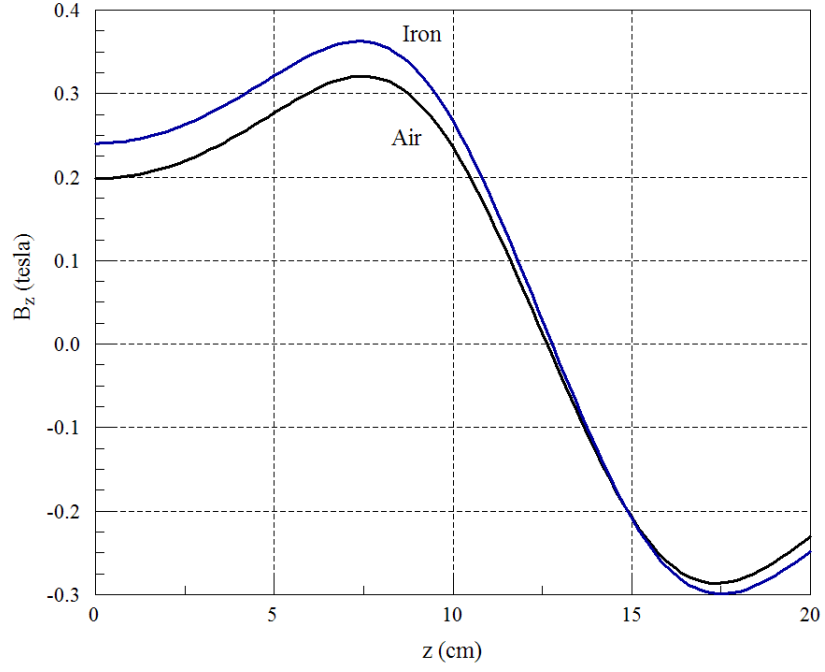


Figure 7: Field variation  $B_z(z, 0)$  for the assembly of Fig. 6. Black trace: bare magnets. Blue trace: iron flux return.

calculation of Fig. 6, the maximum magnitude of magnetic flux density is  $\sim 1.1$  tesla. Typical magnet steels reach saturation at around 2-3 tesla, so the shield thickness could be significantly reduced.